

OPENFSI INTERFACE FOR STRONGLY COUPLED STEADY AND UNSTEADY AEROELASTICITY

C. Valente¹, D. Jones¹, A. Gaitonde¹, J. E. Cooper¹, Y. Lemmens²

¹ University of Bristol
Queen's Building University Walk, Bristol, BS8 1TR, United Kingdom
carmine.valente@bristol.ac.uk

² Siemens Industry Software NV
B-3001 Leuven, Belgium.

Keywords: Fluid-structure, OpenFSI, Aeroelasticity, Coupling, CFD/CSM, Gust.

Abstract: The main objective of this paper is to present the implementation of a new OpenFSI methodology to strongly couple the structural solver MSC Nastran and the CFD code DLR TAU. To achieve this, a dedicated interface has been created to allow both the exchange of information between the two codes and the time synchronization necessary for a strongly coupled analysis. The framework is demonstrated to be a valuable means to accurately simulate steady and unsteady aeroelastic problems. Numerical results obtained from a simulation of an AGARD 445.6 wing example have been used as a benchmark problem to show the applicability of the framework. This framework has then been used for static and gust calculations for the FFAST wing, which is representative of a modern civil transport wing.

1 INTRODUCTION

The current industrial standard for gust loads modelling is to use traditional potential flow models, such as the doublet-lattice method (DLM) and strip theory [1, 2], to generate the air loads interacting with the aircraft structure. However the growing interest in flexible-aircraft dynamics has highlighted how these models make simplifying assumptions that may not allow an accurate prediction of the air loads in these cases.

Since linear unsteady aerodynamics show inaccuracies in the transonic regime, where the linear assumptions are no longer valid and the effects of viscosity and thickness are relevant, many correction techniques have been developed in the past years [3, 4] to attempt to address this issue. Their aim is to introduce wind tunnel data and Computational Fluid Dynamics (CFD) results into the linear unsteady aerodynamics [5, 6] to give improved predictions in this flight regime. Unfortunately most of them rely on a large quantity of additional data.

The increased availability of high performance computing, has seen the development of reliable fluid and structural solvers for use in the engineering design process [7–9]. In the aeroelastic domain, fluid structure interaction procedures are always more often considered as a means to replace expensive experimental campaigns. To solve a computational FSI problem the flow and structural solver have to be coupled with monolithic and partitioned approaches available to compute the solution of this multi-disciplinary problem. The monolithic approach solves the fully discretised system, fluid plus structure, simultaneously,

often requiring a tailored aero-structural solver to be developed. The partitioned approach, on the other hand, makes use of separate solvers for the two domains, allowing existing separate fluid and structural solvers to be used. In a partitioned procedure for fluid structure interaction, the fluid and structural subsystems are time integrated using different schemes, optimised for their different mathematical models, and then they are linked with a numerical algorithm where the synchronisation at each time level must be done iteratively. It is possible to split the methods of coupling the solution into loose, staggered and strong coupling [10].

To answer the need for an analysis environment able to couple fluid and structural loads, an Open Fluid Structure Interaction (OpenFSI) interface has been created, to couple the structural finite element (FE) code MSC Nastran and the CFD code DLR TAU. This interface has been realised using the development environment available within the MSC Software - Solution 400, using the MSC Software Service Development Kit (MSC SDK) [11].

To show the applicability of the developed interface, the AGARD standard aeroelastic configuration for dynamic response, investigated in [12] and analysed in [13, 14], has been studied. A comparison between a loose and strong coupling strategy is shown, as well as the capability to use different types of splining methods to transfer loads and displacements between the aerodynamic and structural models. Following this benchmarking problem, the framework has been applied to the FFAST right wing model [15], a representative model of a general single aisle civil aircraft. The capability to investigate steady aeroelastic problems is first demonstrated through aeroelastic convergence of trim calculations, before an application for a gust load investigation is carried out.

2 FLUID STRUCTURE INTERACTION SIMULATIONS

Fluid structure interaction refers to the situation where a fluid is interacting with a solid structure, exerting force on its surface which may cause displacement of the structure, and as a consequence alter the flow of the fluid itself. The aim of the OpenFSI developed here using the Application Program Interface (API) available in MSC Nastran, is to provide a means to create an interface with a CFD code to allow for fluid structure interaction simulations. The structural and aerodynamic codes will execute simultaneously and exchange information through the OpenFSI interface during the simulation. MSC Nastran reads nodal forces from the external solver and sends structural displacement, velocity and acceleration back to it. The exchange of information is performed on a set of the structural nodes, defined as “wetted nodes”, typically much lower than the number of nodes characteristic of the CFD mesh. An appropriate spline method is required to ensure the correct transfer of the relevant quantities between the different mesh discretizations. In the fluid structure simulation, the CFD code computes viscous and pressure forces, and the relative forces acting on the wetted surface are provided to the FEM code through the OpenFSI interface. On the other side MSC Nastran will compute the displacement, forces and acceleration, based on the driving forces; and the computed quantities of the wetted surface are provided to the CFD code.

The OpenFSI allows the transfer of the following information to the FEM code in INPUT: forces and moment, and obtain in OUTPUT: displacement, velocity and acceleration (translational and rotational).

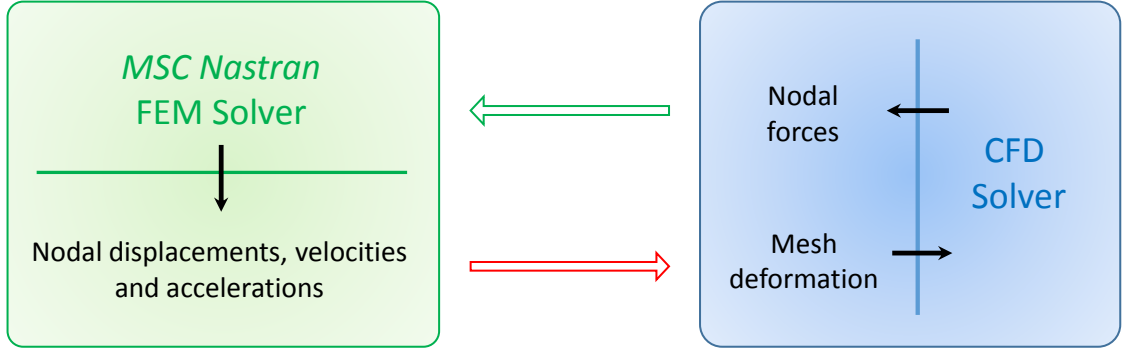


Figure 1: Data exchange in an OpenFSI simulation.

2.1 Coupling schemes

The OpenFSI API interface supports two types of FSI simulations: explicit staggered time steps and implicit coincident time steps. Only the last one has been implemented and will be discussed in this paper.

The implemented method considers coincident time stepping from t^k to t^{k+1} and between the two codes, $\Delta t_F = \Delta t_S$. The FE code solves for convergence within each time step, and the data is communicated between the codes, possibly, multiple times per time step (note that a criteria for maximum iterations may be specified).

The implicit numerical scheme implemented is described in Table 1.

If the numerical scheme performs multiple iterations (Inner Time Steps, index i) for each time step, it is referred to as a “strongly coupled”, otherwise if there is just one inner step, it is called a “loosely coupled” method.

2.1.1 Strong coupling with DLR TAU

To synchronise the time step between the two codes to perform a strongly coupled analysis with TAU, it has been necessary to modify the stream management. The choice of a strongly coupled approach has been necessary to avoid the first order error associated with the time-step, where effectively the structural solution and flow solution are out of sync. TAU is run strongly coupled through initialisation of the variables from two separate streams. One contains the latest solution, the other contains the variables from the (up to) two previous completed time-steps. When TAU initialises the solver for each solution step it reads the variables in the stream from time-level n to $n - 1$ and $n - 1$ to $n - 2$ (if the old variables at $n - 1$ are present in the stream). This step is done only if a deformed grid movement is activated. This step is performed using the stream that contains the data from the last completed time step and then the grid movement is turned off and the latest solution is read in, which overwrites the values in level n (but not those in $n - 1$ or $n - 2$, as grid movement is turned off). In this way the values at $n - 1$ and $n - 2$ are the values from the last completed time step and the values in n are those from the latest solution.

2.2 ALPES OpenFSI Interface

The “ALPESOpenFSI” interface is the name of the interface created using the MSC Software Service Development Kit (SDK) to couple the code TAU by DLR and the FEM



Structure	Fluid
	Step 1: Compute initial force: $f_{F,0}^{k+1} = f_F^k$
	Step 2: Transfer $f_{F,i}^{k+1}$ to the node of the wetted surface: $f_{F,i}^{k+1} \implies f_{W,i}^{k+1}$
Step 3: Get fluid forces on the wetted surfaces from fluid code:	 $f_{W,i}^{k+1}$
Step 4: Structural solver solution for: $(u_{S,i+i}^{k+1}, v_{S,i+i}^{k+1}, a_{S,i+i}^{k+1})$	
Step 5: Send data from the structural solver to the CFD code: $(u_{S,i+i}^{k+1}, v_{S,i+i}^{k+1}, a_{S,i+i}^{k+1}) \implies$	
	Step 6: Update CFD mesh according $u_{S,i+i}^{k+1}$. Solve the fluid subsystem $(v_{F,i+i}^{k+1}, p_{F,i+i}^{k+1})$. Compute the new forces $f_{F,i+i}^{k+1}$.
	Step 7: Increment time i and save the final forces: $f_F^{k+1} = f_{F,i+i}^{k+1}$

Table 1: Implicit fluid-structure coupling, solution scheme.

code MSC Nastran. The service created is an additional piece of code that can be called inside the Nastran bulk data file, and allows a multi-physics analysis FEM/CFD to be performed.

An overview of the ALPESOpenFSI interface solution process is given in Figure 2. To perform a coupled analysis using this interface it is necessary that the FEM and CFD models are coincident in their undeformed (stress-free) configuration, because the displacements that the FEM code computes are evaluated with respect to this configuration. Three main steps can be identified in the solution process:

Initialisation step: at the beginning of the analysis the FEM code sends the CFD information regarding the initial configuration, so that it is possible to prescribe an initial deformation to the models.

Iteration step: the CFD solver sends the computed forces to the FEM solver which will calculate the structural deformation and the associated displacements to apply to the CFD mesh. Two solution approaches have been implemented in the ALPESOpenFSI interface:

Explicit Method: the information is exchanged only once per time step. The forces are read at the beginning of the time step and the displacements are sent at the end of it. During the time step a Newton-Raphson iterative process is used to compute the displacements.

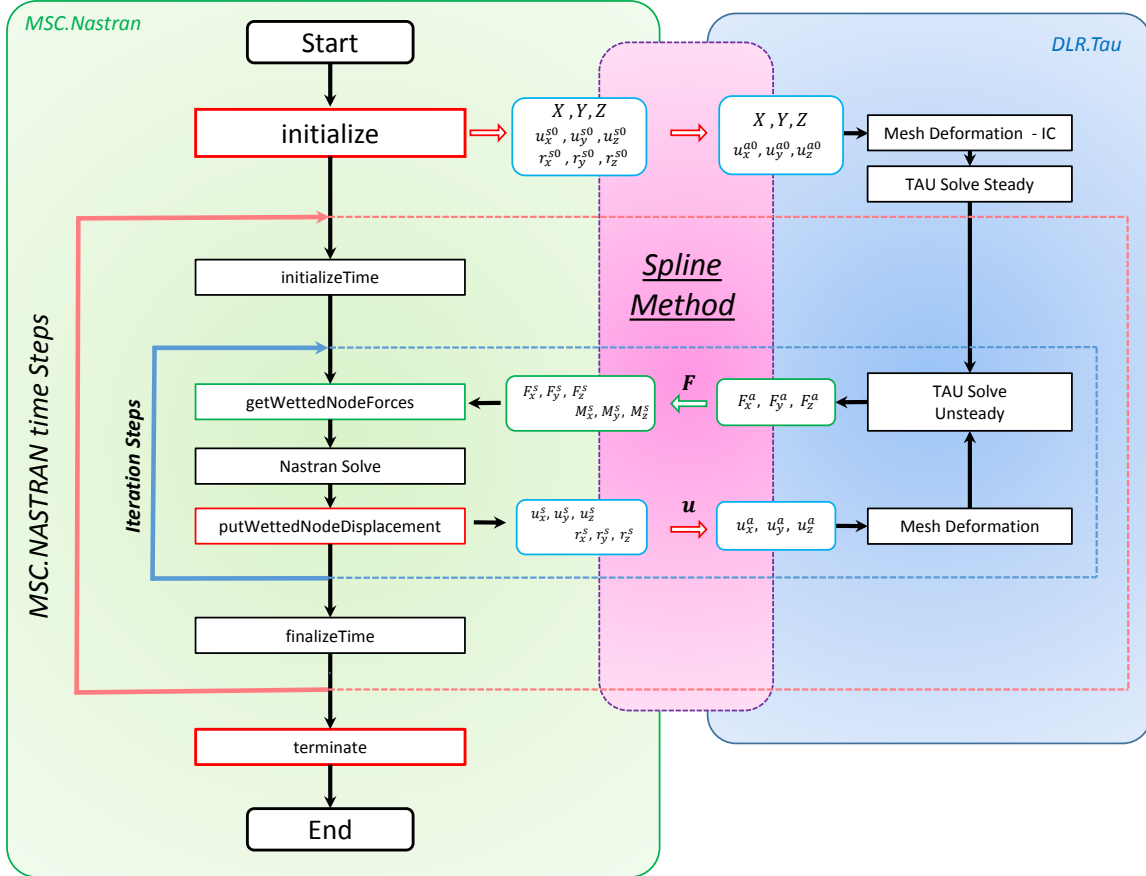


Figure 2: ALPESOpenFSI interface for coupled FEM/CFD simulations.

Implicit Method: the data is communicated inside the Newton-Raphson loop more than once, before exiting from the time step.

Finalise step: at the end of the iterative process a termination message is send to the structural and to the external solver, so that the analysis is terminated and the results file is created [16].

2.3 Nonlinear solution sequence in MSC Nastran, SOL 400

The nonlinear solution sequence available in MSC Nastran, identified as SOL 400, allows the performance of several analysis type combinations, and of particular interest for this research is the nonlinear coupled physics analysis. This is activated when a nonlinear analysis is requested in the case control of the input file. Two nonlinear solutions are available: 1) NLSTAT, nonlinear static analysis, 2) NLTRAN, nonlinear transient analysis. Traditionally most of the coupled fluid structure interaction analysis using an OpenFSI in MSC Nastran have been focussed on the investigation of unsteady problems such as flutter or gust response. The OpenFSI interface is activated in this study for both these cases, together with the capability to perform analysis in multiple steps, where a nonlinear static calculation precedes a nonlinear unsteady calculation. Thus within the same interface the NLSTAT analysis can be used to perform static aeroelastic analysis (e.g. analyse the static aeroelastic deformation of an aircraft, trim analysis), while the NLTRAN analysis can be used to investigate the unsteady response of the structure to a gust disturbance or the two can be combined.

In case of a nonlinear static solution sequence the forces are read at the beginning of the structural solution, and they are transferred to the structure in a series of steps (defined by the user), where the external load increase from 0% to 100%. This is necessary to avoid problems with convergence of the FEM solver, (e.g. in presence of “large displacement”). It is also possible to introduce a relaxation factor to facilitate the convergence to the steady deformation.

2.4 Interpolation method

One of the most important aspects for a fluid structure analysis is how information is transferred between the different models. Most of the time each solver uses a different mesh, in particular due to the different characteristics of the models. The fluid mesh is much more refined compared to the structural one, and most of the time they don't coincide at the fluid-structure interface. However to be able to perform a calculation it is fundamental to transmit the load from the CFD nodes (aerodynamic model) to the finite element nodes (structural model), so that a deformation may be computed and used to update the position of the aerodynamic grid. In order to transfer the forces and displacements from the CFD mesh to the FEM, and vice versa, it is necessary to use a transformation matrix. The ALPESOpenFSI interface is independent from the method used to compute the fluid-structure interpolation matrix. They are read during the initialisation step of the analysis and only matrix-vector multiplications are performed during the analysis step. For this the forces on the structural grid will be obtained via:

$$\mathbf{f}_{str} = \mathbf{H}_{sa} \mathbf{f}_{aero} \quad (1)$$

where \mathbf{H}_{sa} is the force interpolation matrix. The aerodynamic displacement are given as:

$$\mathbf{u}_{aero} = \mathbf{H}_{as} \mathbf{u}_{str} \quad (2)$$

where \mathbf{H}_{as} is the displacement interpolation matrix.

Two different methodologies have been used to obtain the interpolation matrix. The first is an interpolation scheme based on radial basis function, developed by Rendall and Allen within the CFD Group at the University of Bristol [17, 18]. The second method is based on the 3D beam and 3D surface available in MSC Nastran using SPLINE6 and SPLINE7 [19]. The method developed by Rendall and Allen is a method that using radial basis functions (RBFs) works on totally arbitrary point clouds of any form, allowing the removal of all dependency related to volume mesh, structural mesh and flow solver type. This can be achieved because all connectivity requirements are removed from both the coupling and mesh motion problem. Detailed information regarding the implementation are discussed by Rendall and Allen in [17].

One of the advantages of this method is that it can be applied to both structured and unstructured mesh as well as to poor quality meshes where the aerodynamic and structural surface may cross. Despite the totally general formulation and applicability to any mesh type and structural elements, this method can be expensive in terms of memory requirements, since the dimension of the global coupling matrix is $N_s \times N_a$ (where N_s and N_a are respectively the number of surface structural and aerodynamic points). A further improvement of this method from Rendall and Allen [18] has increased the efficiency by using a pointwise partition of unity (PPoU), which has allowed the matrix size to be reduced substantially, without any significant loss in the smoothness of the aerodynamic

surface. In the improved formulation of this method the forces are transferred only to structural points near to each aerodynamic point.

Even though this method allows the conservation of moments and forces, in its current form it is able to transfer only 3 degrees of freedom. For this reason its use is more suitable in the presence of a three dimensional structural model, (e.g. a wing box structure).

The second method used to obtain the coupling has been based on two routines available within the code Nastran, namely SPLINE6 and SPLINE7 which define a six degree of freedom surface and beam spline, respectively. This method, is particular suitable for the situation where the FEM model is represented by beam stick elements. In this particular case the coupling matrix has been obtained using the “Hybrid Static Aeroelasticity Toolkit” [20] developed from MSC Software Toulouse. This toolkit available in the pre-processor MSC Patran Flight Loads, allows a six degree of freedom spline to be generated for fluid structure coupling. The coupling matrix used for this activity has been computed from MSC Software Toulouse.

3 AEROELASTIC TEST CASE

This section presents the results achieved with the ALPESOpenFSI interface for steady and unsteady aeroelastic investigations. First a standard case is considered, the flutter behaviour of the AGARD 445.6 wing. The subsequent test cases are for the FFAST wing, where first a nonlinear static analysis has been used to identify the aeroelastic steady deformation. From this trim configuration a nonlinear unsteady analysis for the gust response has been performed.

3.1 AGARD 445.6 weakened model

The AGARD 445.6 wing model has been chosen as the first aeroelastic test for the ALPESOpenFSI interface. The flutter behaviour of this wing was experimentally investigated by Yates in [12] and numerical computed in many publications [13, 21–23].

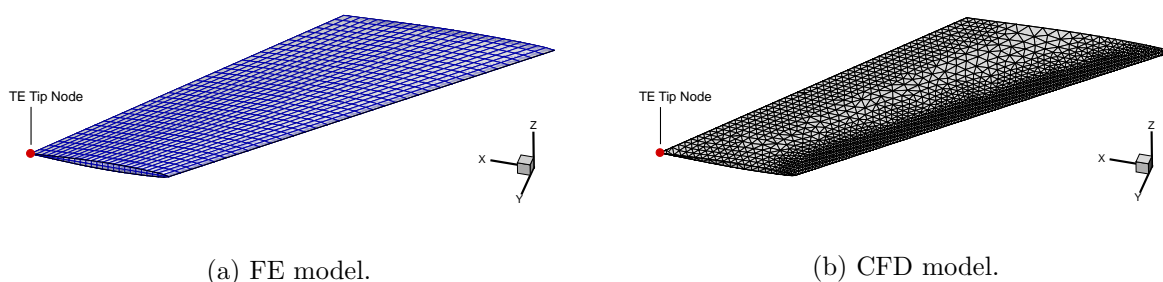


Figure 3: AGARD 445.6 wing model.

The specific configuration selected here is the 2.5 ft weakened model number 3. This model is characterised by a 45° quarter chord sweep angle, a panel aspect ratio of 1.65, a taper ratio of 0.66, and chordwise sections of the wing given by the NACA 65A004 aerofoil. The structural model consist of solid elements, and the material parameter have been designed to give the first five eigenfrequencies. In particular, the first three eigenfrequencies fit those reported in [12] very well.

The coupling surfaces of the aerodynamic and structural mesh are shown in Figure 3. The aerodynamic surface has 3047 grid points leading to 9141 parameters, while the

structural one has 1750 surface grid points leading to 5250 parameters. This model has been analysed in the subsonic case for Mach number $M_\infty = 0.901$, considering a constant density $\rho_\infty = 0.099477 \text{ kg/m}^3$ and an initial dynamic pressure of $p_\infty = 3265 \text{ N/m}^2$. Initially a time step size of $\Delta t = 0.0005$ has been used and the dynamic response of the structure following an initial deflection, proportional to the first bending mode, with a maximum displacement at tip trailing edge of 1 cm , has been studied. The displacement of the tip trailing edge, highlighted in Figure 3 is shown in Figure 4.

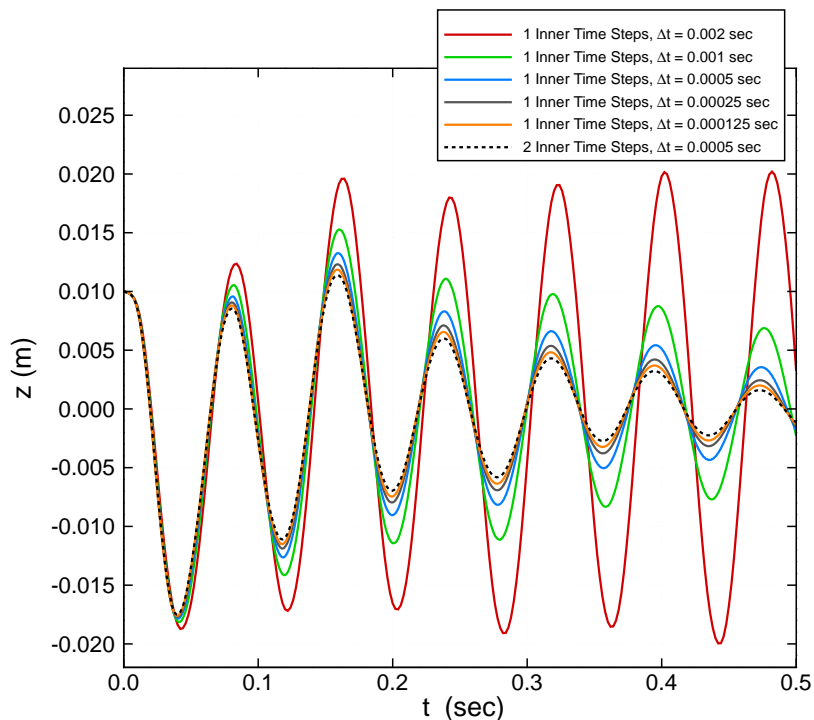


Figure 4: AGARD 445.6 wing tip TE vertical displacement varying time step size, Δt , in a weakly coupled method.

Figure 4 shows a comparison of the vertical displacement of the TE at the wing tip, with varying time step size in a weakly coupled method (1 inner time step). A reference solution calculated using a strongly coupled analysis is also included. It is evident how the dynamic behaviour in a loosely coupled method is quite sensitive to the time step size used for the simulation. In particular it can be seen that as the time step size is reduced, the response is gradually converging to the response obtained with a strongly coupled analysis (this reference case is indicated by the dashed black line). In Figure 5, it is possible to observe, that there is little time step influence on the strongly coupled responses. For this specific case, 2 inner time steps are also shown to be sufficient to get convergence between the aerodynamics and structural codes.

3.2 FFAST Wing model

A second more representative geometry, the FFAST wing, was then studied [15]. The suitability of the method to investigate steady aeroelastic analysis was first considered, before an additional unsteady load analysis was performed. A full aircraft model was developed as part of the FFAST project [15] to be representative of a single-aisle civil jet airliner. The structural model of the aircraft is a beam stick FE model with lumped

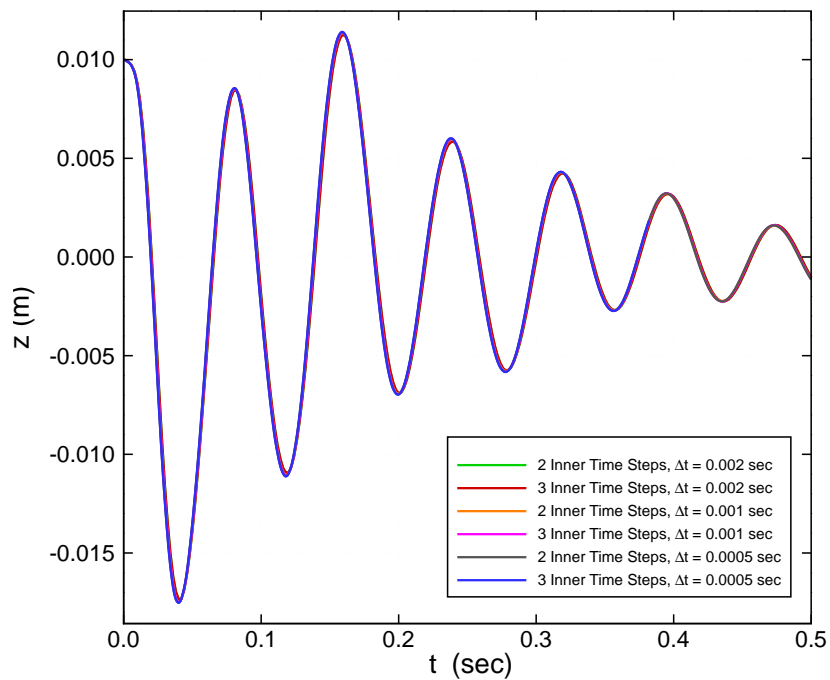


Figure 5: AGARD 445.6 wing tip TE vertical displacement varying time step size, Δt , in a strongly coupled method.

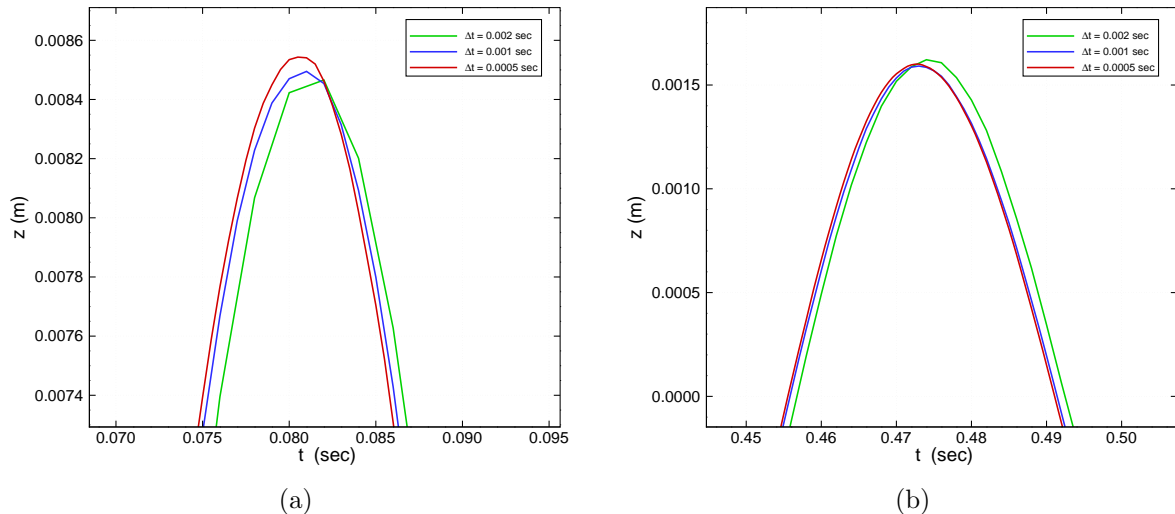


Figure 6: Comparison of TE wing tip vertical displacements, for different Δt using a strongly coupled method with two inner time steps.

masses. For this analysis just the right wing has been considered clamped at the root, and a CFD model has been created using aerofoil data available for the three sections: root, crank and tip. The wing CFD model created does not include the engine and pylon, and has 33227 surface grid points. The FE model contains 10 beam elements for a total of 11 structural grid points. A comparison of the two models is shown in Figure 7.

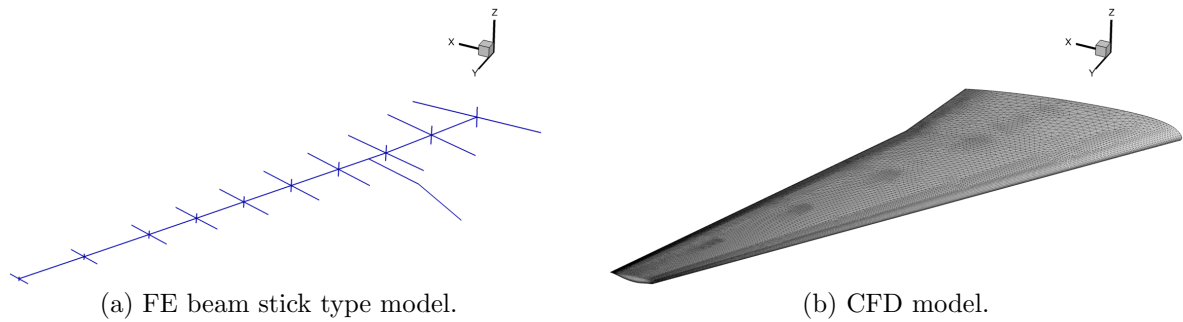


Figure 7: FFAST right wing model.

3.2.1 Aeroelastic Static Trim analysis

The ALPESOpenFSI interface has been used to identify the trim aeroelastic steady deformation. The flight condition chosen to investigate the gust response (see next section) is a $1g$ condition at 11000 m , Mach number $M = 0.85$ and 2° angle of attack. The steady deformation of the wing at trim and the convergence of the vertical displacement of the wing tip is shown in Figure 8. In this case 6 iterations are necessary to get to the steady convergence, and no relaxation factor has been applied.

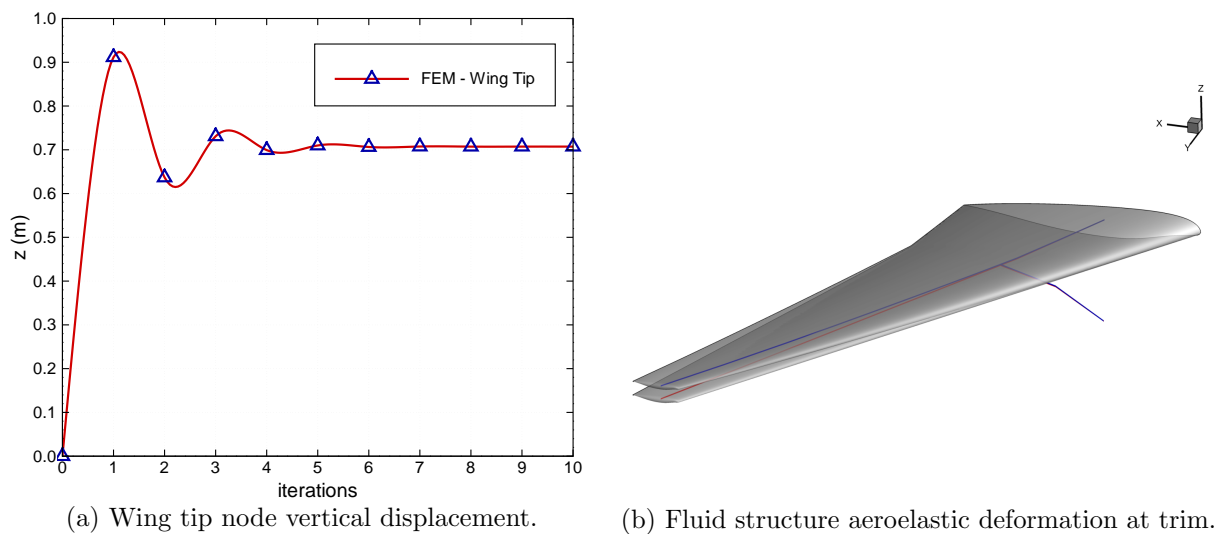


Figure 8: FFAST wing trim analysis.

3.2.2 Unsteady transient analysis for gust

Figure 9 shows a typical one minus cosine (1MC) gust velocity profile, having a maximum gust velocity of w_{g0} and gust wavelength of L_g . As prescribed by the “Certification Specification for Large Aeroplanes CS-25” [24], the shape of the gust has to be taken as:

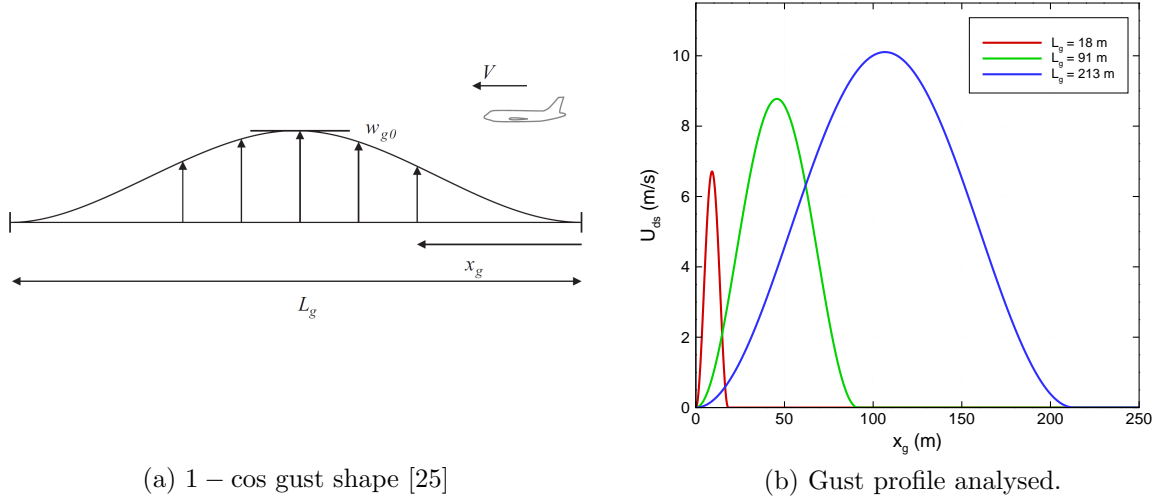


Figure 9: Gust profile.

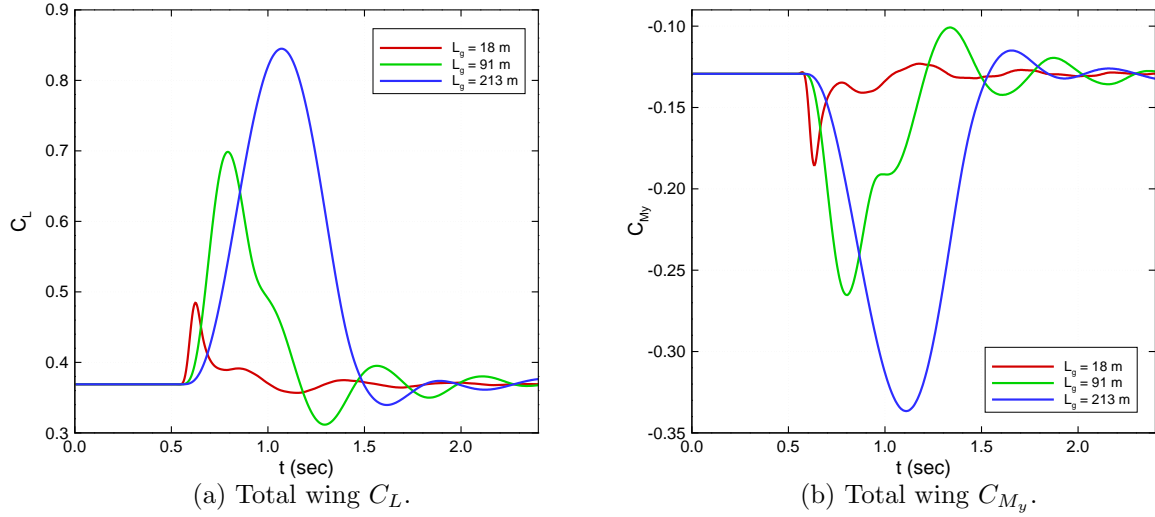


Figure 10: CFD results due to the gust.

$$v_g(x) = \begin{cases} \frac{U_{ds}}{2} \left(1 - \cos\left(\frac{\pi x}{H}\right)\right) & \text{for } 0 \leq x \leq 2H \\ 0 & \text{otherwise} \end{cases} \quad (3)$$

where x is the distance penetrated into the gust, U_{ds} is the design gust velocity in equivalent air speed (EAS), defined by eq. (4), and H (in m) is the distance parallel to the flight path of the aeroplane for the gust to reach its peak velocity ($H = L_g/2$, half of the gust wavelength). The design gust velocity is then defined as:

$$U_{ds} = U_{ref} F_g \left(\frac{H}{106.68}\right)^{1/6} \quad (4)$$

where U_{ref} is the reference gust velocity in EAS and F_g is the flight profile alleviation

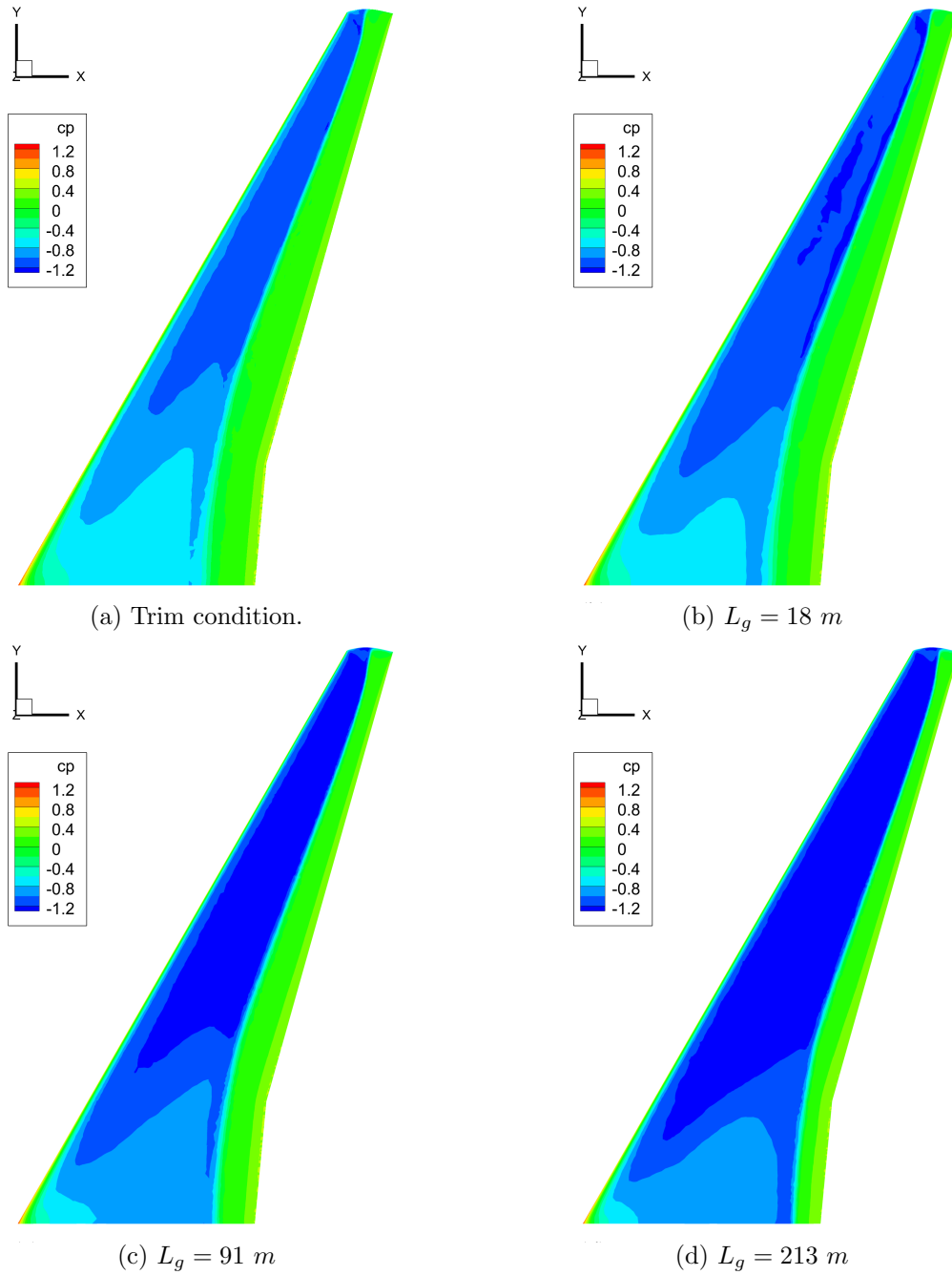


Figure 11: c_p distribution on FFAST right wing upper surface.

factor. U_{ref} reduces linearly from 17.07 m/s EAS at sea level to 13.41 m/s EAS at 4572 m (15000 ft) and then again to 6.36 m/s EAS at 18288 m (60000 ft).

The gust is modelled in TAU, using a field velocity method [26–28]. It is prescribed to start just outside the computational domain and travel at free stream velocity U_∞ . In the following example a value of F_g equal to 1 has been considered. Three reference gust lengths have been analysed and their shapes are depicted in Figure 9. Figure 10 shows the time history of the variation of the global lift and pitching moment coefficient due to the three gust lengths. Figure 11 shows a comparison of the upper wing surface c_p distribution at the trim condition and at the point of maximum lift coefficient after that the gust has perturbed the steady state for the three different gust lengths. The loads at the wing root computed by the structural solver, are presented in Figure 12.

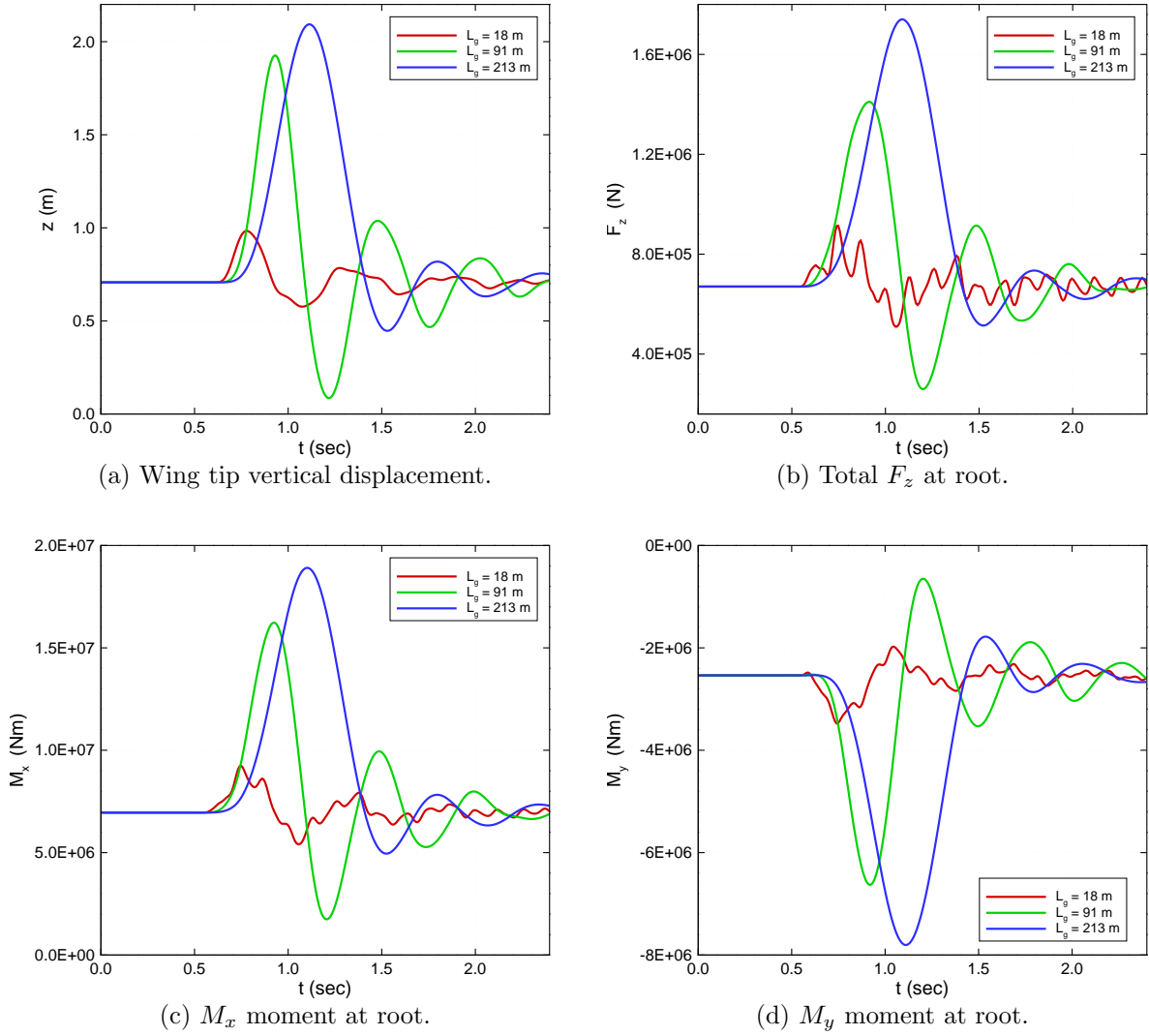


Figure 12: FE model loads resultant at wing root.

4 CONCLUSION

This paper has presented a high fidelity analysis environment to study aeroelastic problems. It consists of a strongly coupled partitioned method that is suitable for the analysis of steady and unsteady aeroelastic problems. The ALPESOpenFSI interface has been realised using the MSC Software SDK and allows the structural code MSC Nastran and the aerodynamic solver DLR TAU to be coupled. Two different approaches to obtain the coupling matrix have been used, and both of them have demonstrated a high level of accuracy in transferring forces and displacements. The advantages of the strongly coupled approach have been demonstrated and discussed for a standard test case close to the flutter speed, where the damping effect plays an important role. An application of more relevance for the flight loads analysis of a generic civil aircraft wing have been presented and discussed. A static aeroelastic analysis is used to identify the trim configuration and the transient nonlinear analysis is used to investigate the loads due to gust events. The stability showed by the coupling scheme is proof that the method can be used to perform loads analysis.

5 NOTATION

f	Force vector
Δt	Time step
t	Time
u	Displacement
v	Velocity
a	Acceleration

Subscript

F	Fluid
S	Structure
W	Nodal quantity on wetted surface
i	Iteration index

Superscript

k	Time step index
-----	-----------------

6 ACKNOWLEDGEMENTS

The research leading to these results has received funding from the European Community's Marie Curie Initial Training Network (ITN) on Aircraft Loads Prediction using Enhanced Simulation (ALPES) FP7-PEOPLE-ITN-GA-2013-607911. The partners in the ALPES ITN are the University of Bristol, Siemens and Airbus Operations Ltd.

7 REFERENCES

- [1] E ALBANO and W P RODDEN. A doublet-lattice method for calculating lift distributions on oscillating surfaces in subsonic flows. *AIAA Journal*, 7(2):279–285, February 1969.
- [2] William P Rodden and Paul F Taylor. Improvements To the Doublet-Lattice Method in MSC Nastran. pages 1–16.
- [3] William P. Rodden, Paul F. Taylor, and Samuel C. McIntosh. Further Refinement of the Subsonic Doublet-Lattice Method, 1998.
- [4] R Palacios, H Climent, a Karlsson, and B Winzell. Assessment of strategies for correcting linear unsteady aerodynamics using CFD or experimental results. *International Forum on Aeroelasticity and Structural Dynamics (IFASD)*, 66(17 2), 2001.
- [5] J P Giesing, T P Kalman, and W P Rodden. Correction Factor Techniques for Improving Aerodynamic Prediction Methods. 1976.
- [6] Jan Brink-Spalink and J. M. Bruns. Correction of unsteady aerodynamic influence coefficients using experimental or CFD data. 2000.
- [7] R Heinrich and N Kroll. Fluid-Structure Coupling for Aerodynamic Analysis and Design – A DLR Perspective. *Most*, (January):1–31, 2008.

- [8] Stefan Keye. Fluid-Structure-Coupled Analysis of a Transport Aircraft and Comparison to Flight Data. In *39th AIAA Fluid Dynamimatics Conference*, number 22-25 June 2009, pages 1–10, San Antonio, Texas, 2009.
- [9] Bernd Stickan, Hans Bleecke, and Silvio Schulze. NASTRAN Based Static CFD-CSM Coupling in FlowSimulator. *Computational Flight Testing Notes on Numerical Fluid Mechanics and Multidisciplinary Design*, 123:223–234, 2013.
- [10] Charbel Farhat, Kristoffer G. van der Zee, and Philippe Geuzaine. Provably second-order time-accurate loosely-coupled solution algorithms for transient nonlinear computational aeroelasticity. *Computer Methods in Applied Mechanics and Engineering*, 195(17-18):1973–2001, 2006.
- [11] MSC Software Development Kit 2014 User’s Guide. 2014.
- [12] E. Carson Yates. *AGARD Standard Aeroelastic Configurations for Dynamic Response. Candidate configuration I - Wing 445.6*. Number 765. 1987.
- [13] Elizabeth M. Lee-Rausch and John T. Batina. Calculation of AGARD Wing 445.6 flutter using Navier-Stokes aerodynamics. (93), 1993.
- [14] K Gupta. Development of a finite element aeroelastic analysis capability. *Journal of Aircraft*, 33(5):995–1002, September 1996.
- [15] Dorian Jones and Ann Gaitonde. Future Fast Methods for Loads Calculations : The FFAST Project. In *Innovation for Sustainable Aviation in a Global Environment proceedings of Aeroday*, pages pp. 110–115.
- [16] MSC Nastran 2014 User Defined Services User’s Guide. 2014.
- [17] T. C. S. Rendall and C. B. Allen. Unified fluid–structure interpolation and mesh motion using radial basis functions. *International Journal for Numerical Methods in Engineering*, 74(October 2007):1519–1559, 2008.
- [18] T. C. S. Rendall and C. B. Allen. Improved radial basic function fluid-structure coupling via efficient localized implementation. *International Journal for Numerical Methods in Engineering*, 78(January):1188–1208, 2009.
- [19] MSC Software. MSC Nastran Quick Reference Guide 2014. 2014.
- [20] MSC Software, F. G. Di Vincenzo, and A. Castrichini. *MSC Nastran Hybrid Static Aeroelasticity Integrated , Accurate Static Aeroelastic Analysis with CFD data*. 2013.
- [21] R Unger, M C Haupt, and P Horst. Coupling techniques for computational non-linear transient aeroelasticity. *Proceedings of the Institution of Mechanical Engineers, Part G: Journal of Aerospace Engineering*, 222(4):435–447, 2008.
- [22] K. Lindhorst, M C Haupt, and P Horst. Usage of time domain surrogate model approaches for transient, nonlinear aerodynamics within aero-structural coupling schemes. In *42nd AIAA Fluid Dynamics Conference and Exhibit*, number June, pages 1–14, New Orleans, Louisiana, 2012.
- [23] Ramji Kamakoti and Wei Shyy. Fluid-structure interaction for aeroelastic applications. *Progress in Aerospace Sciences*, 40(8):535–558, 2004.

- [24] Easa. Certification Specifications for Large Aeroplanes CS-25. Technical Report 19 September, 2007.
- [25] J. R. Wright and J. E. Cooper. *Introduction to Aircraft Aeroelasticity and Loads*. 2007.
- [26] Ralf Heinrich. Comparison of different approaches for gust modeling in the cfd code tau. pages 1–12.
- [27] Gowtham Jeyakumar and Dorian Jones. Aerofoil gust responses in viscous flows using prescribed gust velocities. Technical report, 2013.
- [28] C. Wales, D. Jones, and a. Gaitonde. Prescribed Velocity Method for Simulation of Aerofoil Gust Responses. *Journal of Aircraft*, pages 1–13, 2014.

8 COPYRIGHT STATEMENT

The authors confirm that they, and/or their company or organization, hold copyright on all of the original material included in this paper. The authors also confirm that they have obtained permission, from the copyright holder of any third party material included in this paper, to publish it as part of their paper. The authors confirm that they give permission, or have obtained permission from the copyright holder of this paper, for the publication and distribution of this paper as part of the IFASD 2015 proceedings or as individual off-prints from the proceedings.